14.4

High Resolution Multi-Sensor Profiling of Gust Fronts

Haldun Karan and Kevin Knupp
University of Alabama in Huntsville
Huntsville, AL 35899

1. Introduction

The horizontal pressure gradient due to the high hydrostatic pressure of the cold-dome is basically the source for the gravity or density type of currents. As explained by previous studies, (e. g., Wakimoto 1982; Weckwerth and Wakimoto 1992; Haertel et al. 2001), thunderstorm downdrafts driven by precipitation drag and evaporative cooling of the raindrops are cooled by evaporating precipitation and melting of graupel and hail as they descend. Subsidence and subsequent divergence near the surface underneath the cooling lead the relatively dense air to spread out. The leading edge of the outflow that propagates further ahead of the storm has been termed the *gust front (GF)*.

A total of 32 gust fronts from have been analyzed from data collected by the UAH Mobile Integrated Profiling System (MIPS). The data set includes cases from southeast Texas (during the Texas Air Quality Studies – TEXAQS – between 2 August and 20 September 2000) and the Florida Keys region (during the 4th Convection and Moisture Experiment – CAMEX-4 – between 10 August and 12 September 2001). This paper summarizes the kinematic and thermodynamic properties of a variety of gusts, using the MIPS 915 MHz wind profiler, 2 kHz Doppler sodar, a lidar ceilometer, surface instrumentation and a 12-channel microwave profiling radiometer during CAMEX-4. All gust front cases observed during each program have been analyzed. Section 2 summarizes statistics of all 32 gust front cases, and Section 3 provides details on one gust front case study.

Time of the gust frontal passage is decided based upon the variation in surface thermodynamics and kinematics and also signatures of gust fronts on 915 MHz Doppler radar, sodar and ceilometer. This study also reveals time-height variation of two-minute horizontal wind field and mean vertical velocities and spectral width for some selected cases. Section 2 will give some statistics of the gust fronts observed throughout the two field studies. In section 3, one selected gust front case will be discussed in detail. Summary and conclusion will be presented in section 4.

2. Statistical Characteristics of Observed Gust Fronts

Number of occurrences and statistical characteristics of total of 32 gust fronts are shown in table 1 and Fig. 1, respectively.

	# CBL	# NBL	# TL	TOTAL
KAMP	9	7	2	18
TEXAQS	10	1	3	14
TOTAL	19	8	5	32

Table 1. Number of observed gust fronts during KAMP, and TEXAQS field campaigns. CBL, NBL, and TL are between noon an sunset, between shortly after sunset and sunrise, between sunrise and local noon, respectively.

Most of the gust fronts were sampled during the afternoon and early evening hours. Fig. 1 shows variations of differences in dew point temperature, temperature, mixing ratio, and wind speed prior to and just behind the GF. The differences are taken as absolute values of measurements before the gust front passage, and the peak values after the gust front passage, but before precipitation if any. Vertical velocities are derived from 915 MHz Doppler profiler. Heights of gust frontal heads were subjectively determined from two-minute winds derived from 915 MHz profiler, *SNR,* and spectral width variations. In addition to the 2-min wind fields, localized high spectral width and *SNR* values provided additional information determining gust frontal heights.
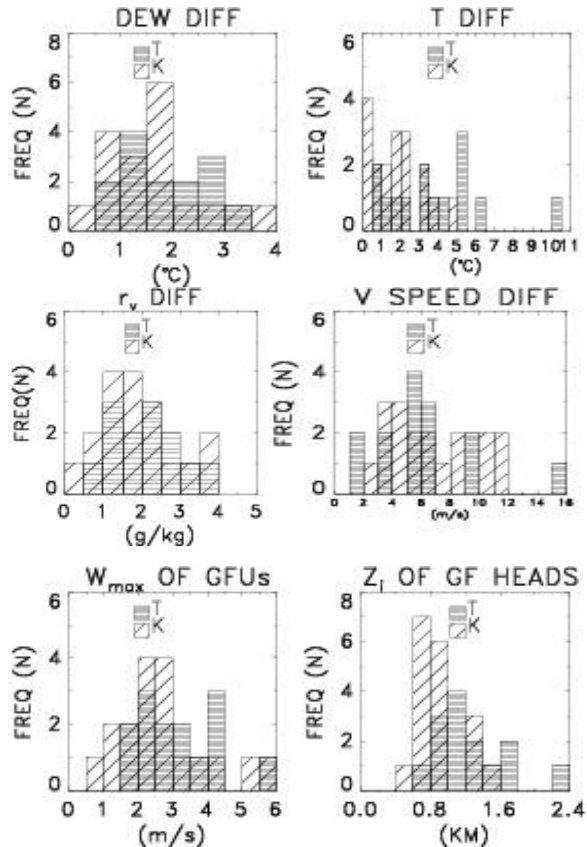
Fig.1. Number of occurrences of changes in temperature, dewpoint, mixing ratio, and wind speeds at surface. Also figure shows statistical variations of gust frontal updrafts, height of heads during the front passage. T and K refer to *TEXAQS* and *KAMP* respectively.

As shown in Fig. 1, wind vector change gustiness varies from 2 to 16 m/s. Temperature and potential temperature usually decreased after the gust front passage, but in a few cases, temperature showed no change or a slight increase (about $0.3°C$-$0.5°C$) during the frontal passage, then decreased sharply. Fig. 1 shows that temperature differences over the Key West, *FL* (a marine setting) were less than they were over the Houston, *TX* (a continental setting). Overall, environmental air over Houston, *TX* was extremely dry. During TEXAQS, dew point depressions for almost all cases were large. Lower relative humidity in the TEXAQS cases affected cloud formation and structure as well.

Based on the ceilometer derived cloud base height information, the Key West region has more favorable environmental conditions to form low-level clouds than Houston, *TX* area. 16 out of 17 cases showed cloud base height less than 1 km during the gust frontal passage. Over the Houston area, cloud base heights less than 1 km occurred only 5 out of 13 cases. Ceilometer return power of 30 dBpW or above is taken as a good indication of cloud base height.

Dew point and mixing ratio variations during the GF passage, on the other hand, don't show much difference between two the regions. Mean vertical velocities of the two regions are about 2-3 m/s. Heights of the gust frontal heads, however, show distinct difference between the two regions. While Z_{head} at *KAMP* are mostly around 600-800 meters, the *TEXAQS* Z_{head} for most cases exceeded 1.2 km. This suggests that cold outflows over *FL* are much shallower than they are at Houston, *TX* .

All the gust front cases exhibited a pressure jump. The speeds of both the environmental air and the outflow reach a minimum value at the gust front. A pressure gradient must be generated to decrease the wind speeds in both sides of the air, as explained by Wakimoto (1982). Our analysis of sodar and 915 profiler revealed that the surface pressure jump was coincident with gust frontal updrafts. The maximum non-hydrostatic pressure jumps among the 32 gust front cases was only about 0.5 mb. A pressure rise starts slowly within the surface wind shift, attains peak values within the high gusty winds. After the gust frontal passage, pressure either continuously increases to the storm's cold dome, or it shows sudden drop just behind the gust frontal updrafts either because of the K-H waves or downdrafts associated with horizontal vortices, and then it rises again.

Ceilometer measurements of cloud base indicate that if gust fronts emanated from thunderstorm outflow as a pure gravity current (i.e., it is not associated with any waves) and if there was no significant prior updrafts), 50% of the gust front cases show clear sky prior to gust front arrival. These cases show either cloud starts to form about

5 to 10 minutes before or right at the time of the gust frontal updrafts.

The vertical bulge near the front of the air mass is called the "GF head." The heights of "heads" are determined by two-minute time-height sections of wind field, which provides kinematics of environmental airflow and cold outflow. We also used the fact that turbulent mixing occurs in the region of a wake of the head. Since 915 MHz Doppler radar return power is proportional to the refractive index structure parameter, C_n^2 - dependent on the moisture and temperature gradient for the clear atmosphere (free of hydrometeors and particles- No rayleigh scattering), very distinct lobes and clefts shape signatures were detected throughout our observations. In addition, mixing behind the KH billows are identified from 915 *SNR* and spectral width products. For this data set, the depths of the heads vary between 0.6 and 2.4 km.

3. August 23, 2000 Case Study

An individual convective cell developed about 75 km NE of the KHGX WSR-88D. Figure 2 shows reflective factors at 1923, and 2013. The *MIPS*
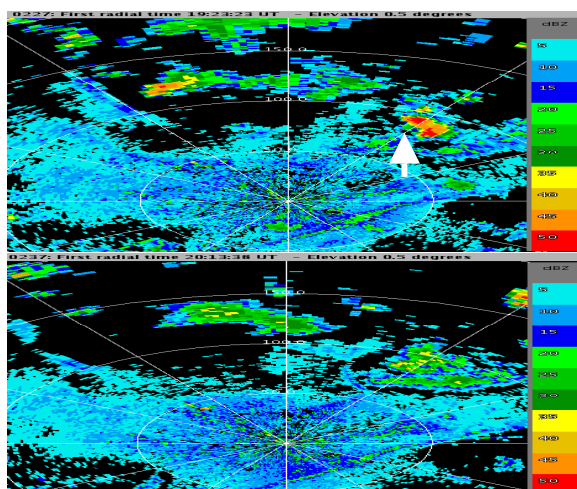

Fig. 2. KHGX WSR-88D 0.5° elevation angle reflectivity factor at 1923 and 2013. *MIPS* location is shown with an arrow at the top left image.

location is depicted with an arrow. The two times,

1923 and 2013 UTC are the first observed updraft time and the starting time of continuous rain, respectively.
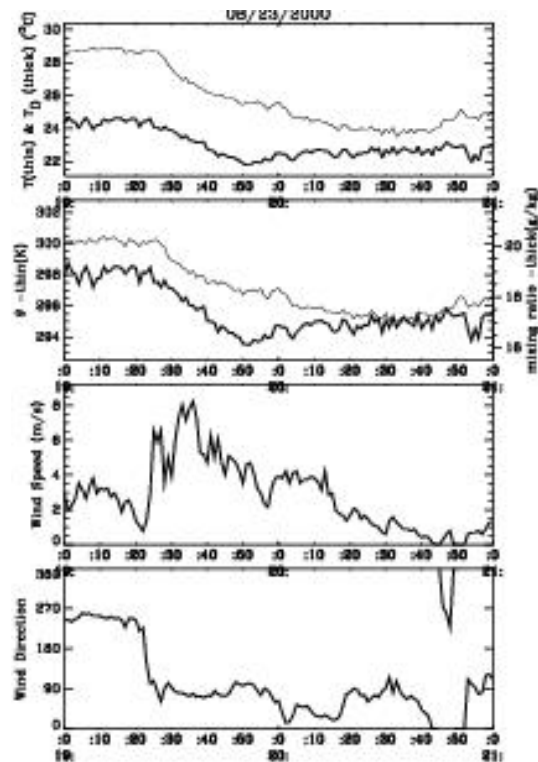

Fig 3. Time series of temperature and dew point temperature, potential temperature (thin) and mixing ratio, wind speed, and wind direction at the surface from 1900 to 2100 UTC on August 23, 2000.

Surface instrument did not record precipitation during the gust frontal passage, nor did ceilometer data indicate precipitation rolls within the gust front. Fig. 3 shows time series of surface thermodynamic and wind variations. Surface thermodynamic variables start falling as the boundary passes. Minimum surface winds of 0.5 m/s occurring at 1922 (all times are in UTC, subtract 5h to get local time) are coincident with convergence and gust frontal updrafts seen at Fig.4. Gusty winds of about 8 m/s existed behind the gust front. The gust front passage was first observed as a surface wind shift starting at 1920. Before the thunderstorm outflow, very weak WSW environmental flow can be seen in Fig. 5. Within the next

couple of minutes after the wind shift, surface instruments recorded minimum wind speed and a slight temperature and potential temperature increase, which were simultaneous with the gust frontal updrafts
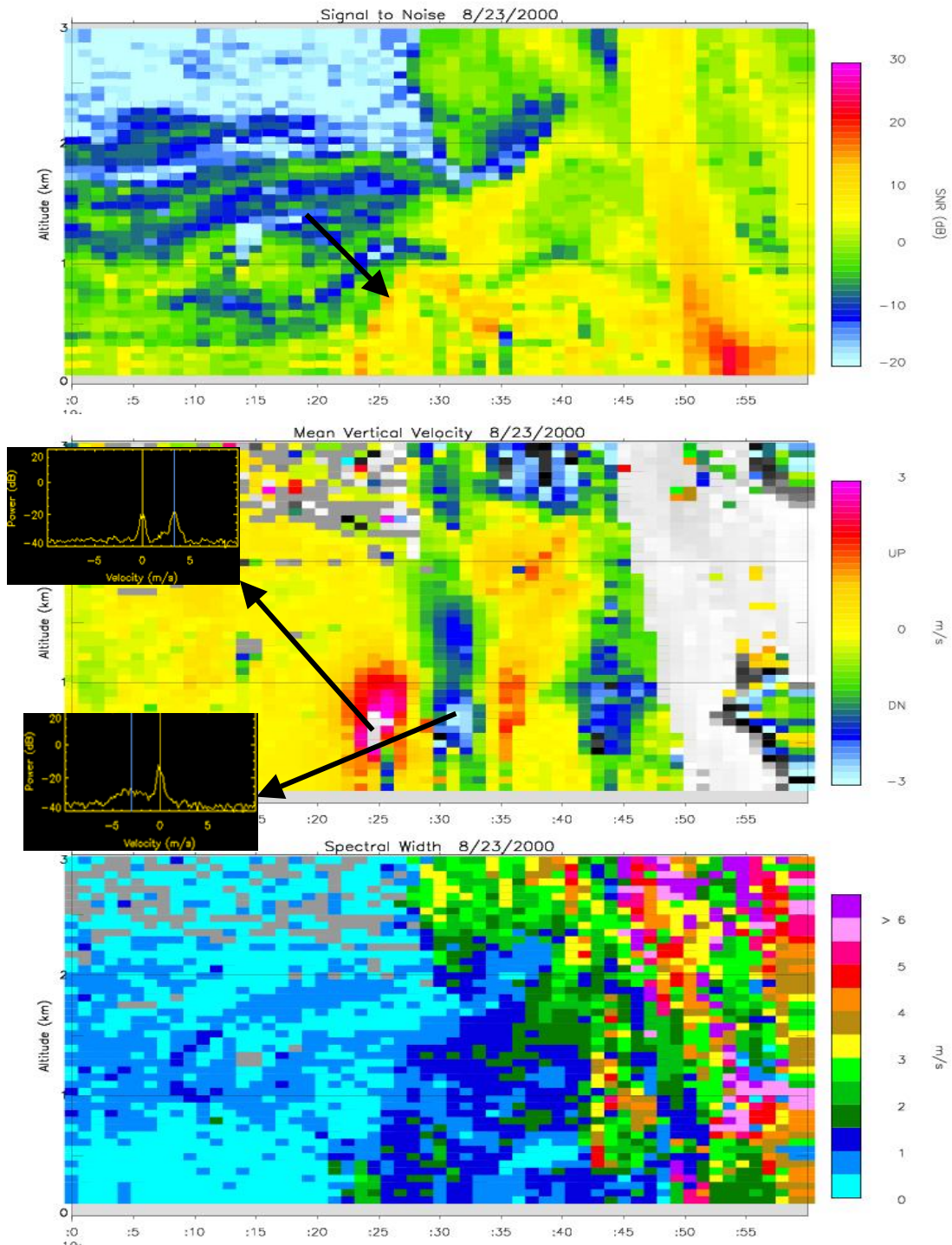

Fig. 4. Time-height cross sections of 915 MHz profiler from 1900 to 2000 on 23 August, 2000. Parameters shown are signal-to-noise ratio (top panel), mean vertical Doppler velocity (middle)- values exceeding the color scale are in gray colors, and Doppler spectrum width (bottom).
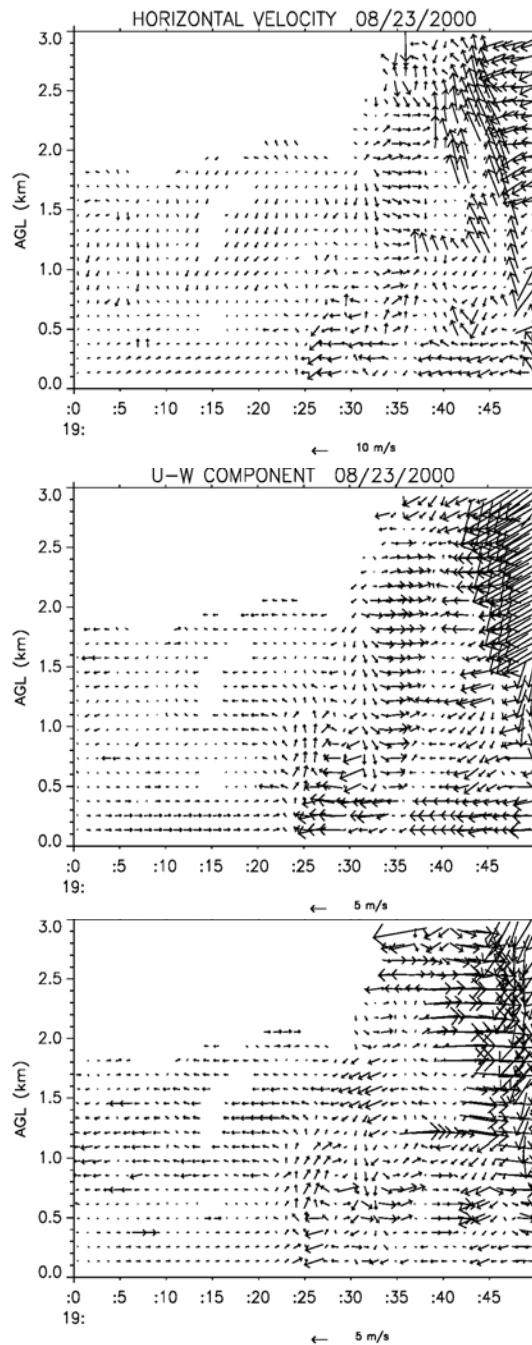
shown in Fig. 4.   Selected two Doppler velocity

Fig. 5.Time-height section of 915 MHz derived 2-min winds from 1900 to 1950 on 23 August, 2000. U-V component (horizontal) of winds (top panel), U-W component of winds (middle), and V-W component of winds (bottom). Wind scale is shown under each figure with 10, 5, and 5 m/s respectively. Winds from left to right represent westerly (southerly) for the middle (bottom) panel.

spectra plots for the maximum and minimum observed vertical velocities show that radial velocities of about +/- 3 m/s toward and away from the profiler. The 2-min averaged wind field of 915 MHz Doppler radar (Fig. 5) shows weak, WSW environmental flow up to 2 km. Easterly flow behind the gust front can clearly be seen from surface to ~700 m.

Careful examination of the timing of minimum surface wind speed and 915 MHz mean vertical velocities reveal that the first wind shift is due to the return flow since the cold outflow arrival has not yet occurred. In addition, the 2-min wind field shows environmental flow is still exist during this time. It also displays elevated outflow protrusion into the environmental flow. This is most clearly seen in the U-W component of wind in Fig. 5 (middle panel). There is about 4 m/s easterly outflow from 1920 to 1924 at 0.5-0.6 km levels. During this period, low levels are still experiencing westerly environmental flow. Laboratory density flow simulations have shown this type of outflow protrusion and elevated updrafts, called gust front nose.

Fig. 4 shows that gust frontal updrafts are coincident with convergence regions shown in Fig. 5, and time of the surface minimum wind speed. Mean vertical velocities are calculated over a 30-second integration interval. Updrafts with 3 m/s or more lasted for about 4 minutes are more pronounced from 0.3 km to 1 km AGL. A strong downward motion exceeding 3m/s follows the gust frontal updrafts. Wind shift ceases right at the beginning of this downdrafts. Easterly cold outflow with gusty winds is present in the lowest 1 km within the wake region of gust front head and 0.5 km atop of the gust front body.

Two distinct up and downdraft couplets shown in Fig. 4 are believed to be generated by Kelvin-Helmholtz instability. Fig. 5 shows two pronounced convergence zone up to 0.5 km at 1924 and 1935. This second convergence maximum is less prominent and   is consistent with weaker (~1.5- 2 m/s) updrafts and following downdrafts.

Some spectral width values (~2-3 m/s) are only visible during the gust frontal updraft and downdraft behind the gust front. Other studies have shown reduced turbulence behind the gust front because of a quasi-unidirectional strong outflow. However, in this case, very low turbulence is associated with the gust front head and wake behind the gust front at upper levels. Higher spectral width values at high altitudes from 1930 to 1950 are believed to be due to not only turbulence but also from variable fall speeds of hydrometeors.

Fig. 4 (top panel) shows wavy thin layers of high signal-to-noise ratios starting at 1923 (shown with an arrow). This wave signature is believed to be associated with KH waves produced by vertical wind shear generation. The KH waves here consist of two waves that take about 10-12 minutes to pass the *MIPS*. Theoretical and observational studies have shown that the lifetime of KH waves is about 10 to 13 minutes (e.g., Muller and Carbone, 1987; Weckwerth and Wakimoto, 1992; May, 1999). We hypothesize that these up and –downdraft couplets are produced by the horizontal vortices associated with KH instabilities.

Strong refractive index gradient, insects, and perhaps wind blown debris at the leading edge of the outflow are the reasons for thin echo lines. For this particular case, it is believed to be due to the combination of both, refractive index gradients and particulates and/or insects. SNR values between 0 and -5 dB prior to the gust front are preceded 15 dB values which mark mostly the warmer environmental side of the interface between environmental air and outflow. Comparison studies on sea breeze fronts (SBF) of onshore vs. offshore (Wakimoto and Atkins, 1994) reveals that onshore SBF becomes harder to identify through the Doppler display than it is for offshore SBF because of their accompanied insect population. But it is not unusual for thin line echoes associated with a gust front to be due to the pure

refractive index fluctuations. Wilson et al. (1994) stated that echoes were resulted from both particulates and Bragg scattering. They found out that particulate scattering dominates in the well-mixed BL (for C-band wavelength), whereas, Bragg scattering dominates at and above the top of the well-mixed BL.
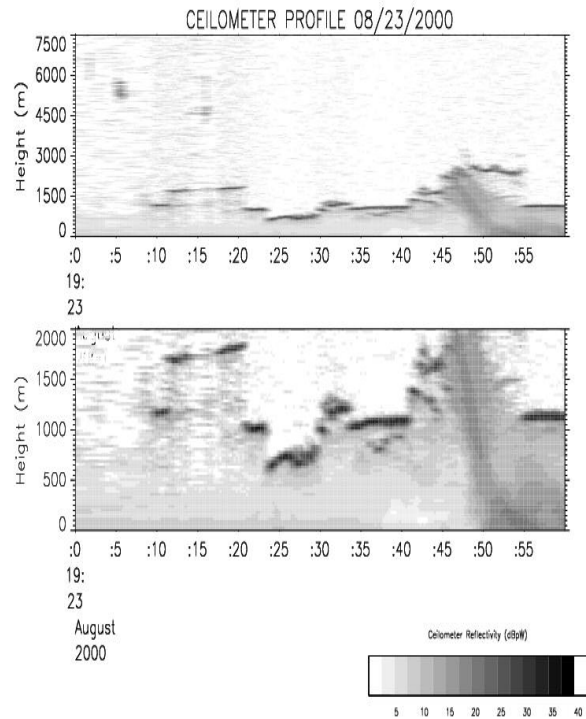

FIG. 6. Time-height section of Ceilometer (Vaisala CT25K) return power in dBpW between 1900 and 2000 on 23 August, 2000. Return power is scaled from 0 to 40 dBpW.

Careful examination of 915-*SNR*, 2-min wind field, and ceilometer data reveal that thin line echoes within, above, and behind the gust front are most likely produced by refractive index turbulence which is a function of C_n^2, dependent on moisture and to a lesser extent on temperature gradients. Ceilometer return power is extremely weak during the gust front passage, yet 915 *SNR* values are quite large. Based on these arguments, we believe that the C_n^2 gradient contribution dominates the Rayleigh scatter contribution on 915-*SNR.* The first crest of KH wave is located at 1 km at about 1928, and the first

trough is at 0.5 km at 1933 with 15 dB SNR values. Fig. 4 shows easterly outflow reaching up to 0.9-1.0 km at around 1928 and above that altitude there are very weak westerly and/or southerly winds. This boundary is marked with higher echoes. The second crest of KH waves is marked with relatively weaker echoes (~10 dB). Again, these return echoes are coincident with the boundary between outflow and environmental flow. Also notice strong vertical wind shear along the KH waves.

Continuous clouds exist from 1910 until precipitation arrival (1950). Cloud base height varies between 1.5 km and 0.6 km (Fig. 6). A cloud base height decrease is clearly seen at the figure at around 1922 at which strong updrafts occurred. Before this time, cloud base height is about 1-1.5 km then it decreases down to 0.6 km and rises up to 1 km after the gust front. This type of "U"-shape cloud-base height variation on time-height plots during the passage of gust front was observed in our many gust front cases. The lifting condensation level is altered when *MIPS* experiences differences in temperature and dew point temperature. Fig. 6 shows lowered cloud base after 1925. This time is coincident with arrival of cold outflow (see Fig. 5). Surface observations also show 6 m/s gusty winds right at 1925. They also show temperature and dew point drops which is more abrupt for temperature. So this might explain why LCL is lowered right behind the gust front that is temperature drop is more pronounce than dew changes which leads to lower LCL.

4. CONCLUSION

Gust frontal analysis over two different regions has been conducted with surface observations and ground based remote sensing *MIPS* instruments. Dew point variations over the two regions revealed similar variations as gust fronts pass by the *MIPS*. Dew point temperatures and mixing ratios either increase slightly or decreases unlike the temperature. Before the sudden drop in temperature, in some cases, it shows slight, short lasted temperature increases during the frontal passage. This type of temperature increase has been reported in undular bore, gravity wave studies. Surface wind speed gust (wind surge) right after the frontal boundary varies about 4 to 12 m/s without any significant differences over the two regions. Vertical velocity maximum derived from the 915 MHz Doppler radar are about 2-3 m/s most of the time, and it gets as much as 5 to 6 m/s for some cases.

High-resolution wind field derived from 915 MHz Doppler radar performs very well to delineate the boundary between the storm outflow and environmental flow. Height of the gust frontal head defined subjectively by using turbulence, 2-min wind field and *SNR* information, on the other hand, shows very distinct feature at the two regions. Over the Key West, FL, almost all cases produced head height less than a kilometer. Height of the gust frontal head over Houston, TX region occurred above 1 km mostly. Deep cooling would increase the cold outflow depth and create higher gust frontal head. Outflow depth over Key West, FL region seems to be shallower because of the higher relative humidity of the region and have favorable conditions to reach LCL more quickly.

Surface minimum wind speed is observed to be coincident with convergence zone observed from 915 2-min wind field. Secondary updraft/downdraft and associated circulation have been shown to be related to the low level divergence field and K-H waves. K-H wave type signature is quite obvious on time-height section of *SNR* data. Two updraft/downdraft couples are created in the rotor type circulation environment with the strongest one occurring within the gust frontal boundary.

915 MHz spectral width data shows slight increase in turbulence within the gust frontal zone. The turbulence is associated with thunderstorm outflow with interaction of environmental flow. Most of the cases show moderate to strong turbulence at and behind the gust frontal head, in the wake region atop cold outflow. This case, on the other hand, clearly shows how this structure can be change

substantially. In this gust frontal example, there were no turbulence created due to the colliding flows. This is mostly because of the extremely calm environmental flow conditions.

Cloud base height based on 32 gust front cases decreases with approaching GF, then it increases or stays the same as GF passes by. Key West, FL gust frontal cases have much lower cloud base heights than they are in Houston, TX. Key West, FL region, the environment is much moister than it is in Houston, TX. The air parcel needs more time to reach LCL level (~ higher altitude) over Houston, TX region.

Ceilometer return power for over all cases is somewhat different at two regions. At Key West region, the return power values within the gust frontal boundary below the cloud base were somewhere around 25-30 dBpW while over Houston, they were about 7-10 dBpW. Microwave radiometer data generally show increase liquid water content in the lowest 1-1.5 km from 0.1 gr/kg to 0.6 g/kg during the passage of the gust front. Unfortunately, Microwave radiometer was not available during the *TEXAQS* field project.

REFERENCES

Haertel, P. T., R. H. Johnson, S. N. Tulich, 2001: Some simple simulations of thunderstorm outflows. *J. Atmos. Sci.,* **58**, 504-516.

May, P. T., 1999: thermodynamic and vertical velocity structure of two gust fronts observed with a wind profile/RASS during MCTEX. *Mon. Wea. Rev.,* **127**, 1796-1807.

Mueller, C. K., R. E. Carbone, 1987: Dynamics of a thunderstorm outflow. *J. Atmos. Sci.,* **44**, 1879-1898.

Wakimoto, R. M., 1982: the life cycle of thunderstorm gust fronts as viewed with Doppler radar and Rawinsonde data. *Mon. Wea. Rev.,* **110**, 1060-1082.

—, N. T. Atkins, 1994: observations of the sea-breeze front during CaPE. Part I: Single-Doppler, satellite, and cloud photogrammetry analysis. *Mon. Wea. Rev.,* **122**, 1092-1114.

Weckwerth, T. M., R. M. Wakimoto, 1992: The initiation and organization of convective cells atop a cold-air outflow boundary. *Mon. Wea. Rev.,* **120**, 2169-2187.

Wilson, J. W., T. M. Weckwerth, J. Vivekanandan, R. M. Wakimoto, R. W. Russell, 1994: Boundary layer clear-air radar echoes: Origins of echoes and accuracy of derived winds. *J. Atmos. Oceanic Technol.,* 11, 1184-1206.